Non-Uniform Phase Synthesis for Cosecant-Squared Radiation Patterns

Pedro A. B. Leão, Tcharles V. B. Faria
Graduate Program in Electrical Engineering
Federal University of Minas Gerais
Belo Horizonte, MG, Brazil
pedrobessaleao@ufmg.br, tcharlesdefaria@ufmg.br

Fernando J. S. Moreira
Department of Electronics Engineering
Federal University of Minas Gerais
Belo Horizonte, MG, Brazil
fernandomoreira@ufmg.br

***Abstract*—This work presents the development of an analytical technique for the synthesis of non-uniform phase distribution for a cylindrical aperture with a cosecant-squared radiation pattern. Analytical results for the phase distributions are presented. Using the Aperture Method, the radiation patterns for these distributions are computationally calculated.**

***Index Terms*—Non-Uniform Phase Distribution, Cosecant-Squared, Aperture Method, Reflector Antennas.**

I. Introduction

Cosecant-squared radiation patterns are important for airborne surveillance radar and mobile communications applications. This pattern compensates for propagation losses, meaning that antennas with this characteristic provide greater directivity in the direction with longer propagation paths [1].

There are several works that address the synthesis of antennas with cosecant-squared patterns. Noteworthy methods for improving antenna efficiency are presented in [2], where studies related to the reduction of sidelobes in a cosecant-squared radiation pattern are presented. Additionally, there are works that utilize optimization algorithms of this pattern [3].

It is worth noting, among the antenna models that meet the cosecant-squared pattern, the double reflector antennas for omnidirectional coverage. In [4], an alternative method for the synthesis of this type of antenna is presented. In [5], a high-performance double reflector antenna is also presented.

One way to design an antenna that meets the desired specifications is through aperture field synthesis. In [6], a method for non-uniform phase synthesis is presented, which generates cosecant-squared radiation patterns. However, the author does not provide an analytical solution for this distribution.

Building on the work presented in [6], this study conducts an analytical solution for the non-uniform phase distribution. The analysis is done considering a cylindrical aperture, as it is interesting for applications related to cosecant-squared radiation patterns with omnidirectional coverage. Fig. 1 schematically shows an omnidirectional coverage, with a cosecant-squared radiation pattern and a cylindrical aperture with a height of W_A.

This paper is divided as follows: Section II presents the method of non-uniform phase synthesis; Section III presents the analytical solution for the aperture phase distribution; Section IV presents the aperture method; Section V presents the results, and Section VI presents the conclusions.

This work was partially financed by CAPES, CNPq-303257/2022-9 and FAPEMIG-PPM-384-18.

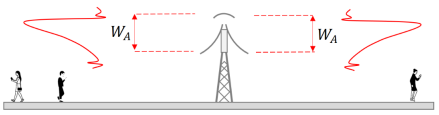

Fig. 1. Representation of the cosecant-squared radiation pattern.

II. Non-Uniform Phase Synthesis Method

The non-uniform phase synthesis method, presented in [6], consists of defining functions $g(\xi)$ and $h(u)$. Function $g(\xi)$ is defined as the power at the cylindrical aperture:

$$g(\xi) = \frac{\int_{-1}^{\xi} |\vec{E}_A(\vec{r}_A, \omega)|^2 \, d\eta}{\int_{-1}^{1} |\vec{E}_A(\vec{r}_A, \omega)|^2 \, d\eta} \tag{1}$$

where $\vec{E}_A(\vec{r}_A, \omega)$ is the aperture field. Following [6]:

$$|\vec{E}_A(\vec{r}_A, \omega)|^2 = 1, -1 \leq \xi \leq 1 \tag{2}$$

From (2), it is understood that the squared modulus of the electric field at the cylindrical aperture is equal to 1 for the entire aperture. It is worth noting that ξ is the normalized aperture coordinate and is given by $\xi = 2\,z/W_A$, where W_A is the height of the aperture.

On the other hand, it is necessary to define the function $h(u)$, which represents the desired radiated power:

$$h(u) = \frac{\int_{-1}^{u} |F_{norm}(\tau)|^2 \, d\tau}{\int_{-1}^{1} |F_{norm}(\tau)|^2 \, d\tau} \tag{3}$$

In [6], $F_{norm}(u)$ is expressed as follows:

$$F_{norm}(u) = \begin{cases} 0, & -1 \leq u \leq u_1 \\ A/u, & u_1 < u < u_2 \\ 0, & u_2 \leq u \leq 1 \end{cases} \tag{4}$$

where $u_1 = \sin(\theta_1 - 3\pi/2)$, $u_2 = \sin(\theta_2 - 3\pi/2)$ and $u = \sin(\theta - 3\pi/2)$. The angles θ_1 and θ_2 are the starting and ending angles of the cosecant-squared pattern. The functions $g(\xi)$ and

979-8-3503-2067-1/23/$31.00 ©2023 IEEE

$h(u)$ have analytical solutions, shown in Section III. The next step is to impose energy conservation:

$$h(u) = g(\xi) \tag{5}$$

By imposing this equality, we then have as a result a function $u(\xi)$. Finally, the last step is to apply the function $u(\xi)$ in (6) [6]:

$$\frac{d\psi(\xi)}{d\xi} = -k\frac{W_A}{2}u(\xi) \tag{6}$$

where $k = 2\pi/\lambda$ and $\psi(\xi)$ is the desired aperture phase distribution. Schematically, Fig. 2 presents the non-uniform phase synthesis procedure presented in [6]. The contribution of this work is to present the analytical solution for the non-uniform phase of a cylindrical aperture, that is, to determine the function $\psi(\xi)$ that provides a cosecant-squared radiation pattern.

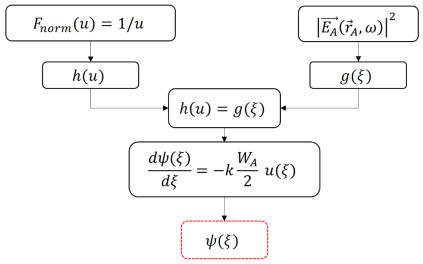

Fig. 2. Synthesis method flowchart.

III. Analytical Solution for Non-Uniform Phase Distribution

Based on (3) and (4), the analytical solution for $h(u)$, which represents the desired radiated power, is given by:

$$h(u) = \frac{u_2\,(u - u_1)}{u\,(u_2 - u_1)} \tag{7}$$

The solution for the required power in the aperture, is expressed with the aid of (1) and (2) as:

$$g(\xi) = \frac{1+\xi}{2} \tag{8}$$

for $-1 \leq \xi \leq 1$. By setting $g(\xi)$ equal to $h(u)$, the function $u(\xi)$ is obtained:

$$u(\xi) = \frac{2u_1u_2}{u_2 + u_1 - \xi(u_2 - u_1)} \tag{9}$$

Analytically evaluating (6) and (9) yields:

$$\psi(\xi) = \left(\frac{kW_Au_1u_2}{u_2 - u_1}\right)\ln\left[u_2 + u_1 - \xi(u_2 - u_1)\right] \tag{10}$$

It is worth noting that the phase distribution $\psi(\xi)$ is dependent on the aperture height W_A and the parameters u_1 and u_2, which are related to the starting and ending angles of the cosecant-squared pattern. In Section V, the behavior of the phase distribution in relation to these parameters will be investigated.

IV. Aperture Method

One can use the Aperture Method, discussed in [7] to evaluate the radiation pattern provided by $\psi(\xi)$. Considering a cylindrical aperture, it can be shown that the ϕ component of the electric field is zero, $E_\phi(\vec{r},\omega) = 0$, and the θ component of the electric field is described as:

$$E_\theta(\vec{r},\omega) \approx -\frac{jk\rho_A}{2}\frac{\exp(-jkr)}{r}\left[\sin\theta\,\mathrm{J}_0(k\rho_A\sin\theta)\right.$$
$$\left.+j\mathrm{J}_1(k\rho_A\sin\theta)\right] \times \int_{-W_A/2}^{W_A/2}\exp[jkz'\cos\theta]\exp[j\psi(\xi)]\,dz' \tag{11}$$

where J_0 and J_1 are the usual Bessel functions and ρ_A is the radius of the cylindrical aperture.

V. Results

Initially, the study of $\psi(\xi)$ as a function of W_A is performed. In Fig. 3, the phase distributions for different values of angles θ_2 are represented. It is worth noting that θ_1 was fixed at $92°$. In this case, W_A was defined as 90λ, that is, the phase distributions must vary in z from -45λ to 45λ. The phase function ψ is given in degrees. It is important to remember that the results using the analytical solution presented in 10 are the same when 6 is numerically solved [6].

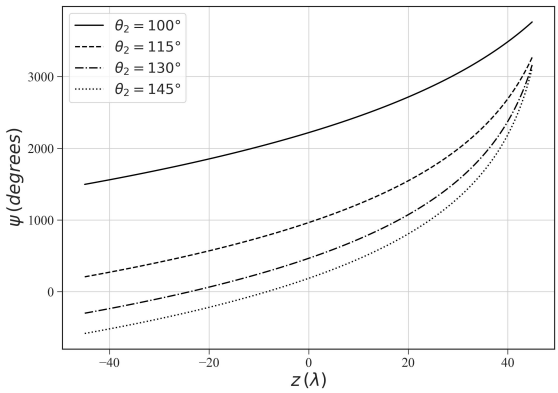

Fig. 3. Non-uniform phase distribution for $W_A = 90\lambda$.

To validate the phase distributions $\psi(\xi)$, the aperture method was computationally implemented. Fig. 4 shows the normalized directivity for the respective phase distributions with $\rho_A = 500\lambda$. In the figure, one can also observe the influence of the angle θ_2 on the width of the cosecant-squared pattern. The dashed curve represents a theoretical pattern, considering $\theta_1 = 92°$ and $\theta_2 = 145°$.

Next, the analysis was repeated for $W_A = 300\lambda$. Fig. 5 shows the phase distributions for different angles θ_2, with $\theta_1 = 92°$. Once again, the directivity was computationally calculated using the aperture method. Through Fig. 6, it can be noticed that the radiation patterns in this case are more directive and closer to the ideal cosecant-squared profile.

Finally, the influence of the radius of the cylindrical aperture ρ_A was evaluated. W_A was fixed at 300λ, θ_1 at $92°$, θ_2 at $115°$, and ρ_A was assigned values of 5λ and 500λ. The results

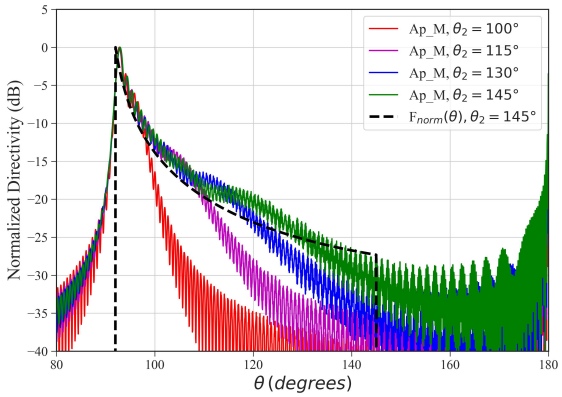

Fig. 4. Radiation pattern for $W_A = 90\lambda$ and $\theta_1 = 92°$.

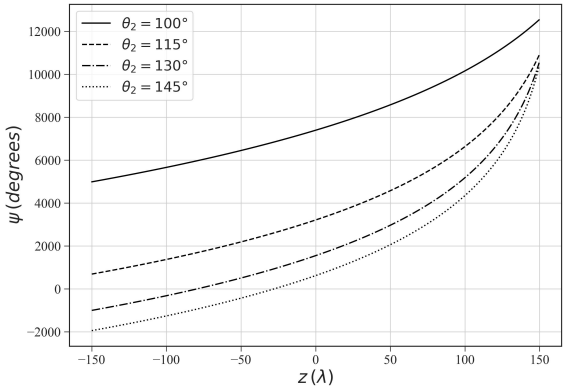

Fig. 5. Non-uniform phase distribution for $W_A = 300\lambda$.

are presented in Fig. 7. The dashed line represents the ideal cosecant-squared profile. For the values of ρ_A evaluated, little influence of the radius of the cylindrical aperture was observed on the radiation pattern.

It is worth noting that with the increase in operating frequencies of mobile communication networks, antennas with aperture dimensions of 300λ are becoming possible to be constructed and commercially available. For example, for a

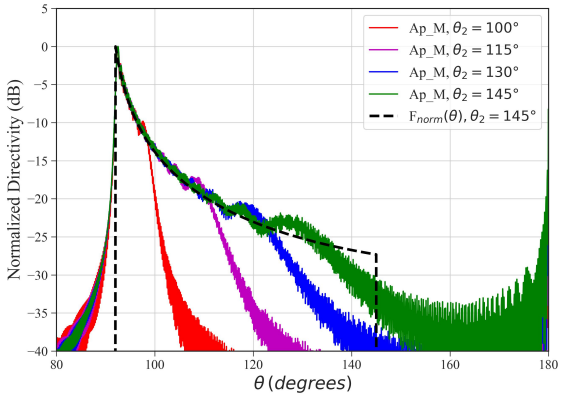

Fig. 6. Radiation pattern for $W_A = 300\lambda$ and $\theta_1 = 92°$.

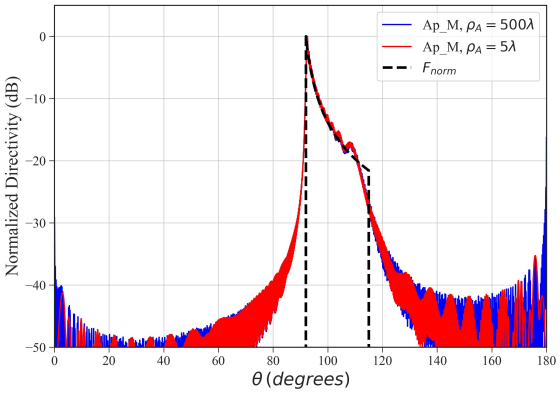

Fig. 7. Radiation pattern for variations in ρ_A.

$W_A = 300\lambda$, a length of 3.4 meters is obtained for 26 GHz 5G network applications. The trend is for these dimensions to become even smaller in the next generations of mobile networks.

VI. Conclusions

This work presented the development of a non-uniform phase synthesis for a cylindrical aperture, considering a cosecant-squared radiation pattern. Results of phase distributions as a function of position on the aperture were presented, as well as the radiation patterns generated by such distributions. An analysis was also presented on the influence of the aperture radius on the radiation pattern. As future work, the presented method will be applied for the synthesis of reflector antennas with omnidirectional coverage.

References

[1] Z. -C. Hao and M. He, *"Developing Millimeter-Wave Planar Antenna With a Cosecant Squared Pattern,"* in IEEE Transactions on Antennas and Propagation, vol. 65, no. 10, pp. 5565-5570, Oct. 2017, doi: 10.1109/TAP.2017.2735460.

[2] H. Chu, P. Li and Y. -X. Guo, *"A Beam-Shaping Feeding Network in Series Configuration for Antenna Array With Cosecant-Square Pattern and Low Sidelobes,"* in IEEE Antennas and Wireless Propagation Letters, vol. 18, no. 4, pp. 742-746, April 2019, doi: 10.1109/LAWP.2019.2901948.

[3] D. Zhao et al., *"Synthesis of Cosecant Squared Pattern based on Convex Optimization,"* 2019 International Applied Computational Electromagnetics Society Symposium - China (ACES), Nanjing, China, 2019, pp. 1-2, doi: 10.23919/ACES48530.2019.9060598.

[4] R. A. Penchel, J. R. Bergmann and F. J. S. Moreira, *"Main-Reflector Shaping of Omnidirectional Dual Reflectors Using Local Conic Sections,"* in IEEE Transactions on Antennas and Propagation, vol. 61, no. 8, pp. 4379-4383, Aug. 2013, doi: 10.1109/TAP.2013.2261571.

[5] R. A. Santos, R. A. Penchel, C. S. Arismar and J. F. Mologni, *"High-performance omnidirectional dual-reflector antenna based on a dieletric subrefletor support,"* 2015 SBMO/IEEE MTT-S International Microwave and Optoelectronics Conference (IMOC), Porto de Galinhas, Brazil, 2015, pp. 1-5, doi: 10.1109/IMOC.2015.7369127.

[6] Biswas, Mahmud. *"An Aperture Synthesis Technique for Cylindrical Printed Lens/Transmit array Antennas with Shaped Beams."* PhD diss., Université d'Ottawa/University of Ottawa, 2013.

[7] C. A. Balanis, *Antenna Theory: Analysis and Design* , 4th edition, John Wiley & Sons, 2016.